Since January 2020 Elsevier has created a COVID-19 resource centre with free information in English and Mandarin on the novel coronavirus COVID-19. The COVID-19 resource centre is hosted on Elsevier Connect, the company's public news and information website.

Molecular Immunology 147 (2022) 199–208

Contents lists available at ScienceDirect

Molecular Immunology

journal homepage: www.elsevier.com/locate/molimm

Influence of SARS-CoV-2 inactivation by different chemical reagents on the humoral response evaluated in a murine model

Emerson de Castro Barbosa [a,e], Adriana de Souza Andrade [a], Myrian Morato Duarte [e], Gilson Faria [a], Felipe Campos de Melo Iani [e], Ana Caroline Zampiroli Ataide [a], Lucas Maciel Cunha [b], Clara Guerra Duarte [c], Sílvia Ligorio Fialho [d], Sérgio Caldas [a,*]

[a] Serviço de Biotecnologia e Saúde, Diretoria de Pesquisa e Desenvolvimento, Fundação Ezequiel Dias, Belo Horizonte, MG, 30510010, Brazil
[b] Diretoria de Pesquisa e Desenvolvimento, Fundação Ezequiel Dias, Belo Horizonte, MG, Brazil
[c] Serviço de Toxinologia Molecular, Diretoria de Pesquisa e Desenvolvimento, Fundação Ezequiel Dias, Belo Horizonte, MG, Brazil
[d] Serviço de Desenvolvimento Tecnológico Farmacêutico, Diretoria de Pesquisa e Desenvolvimento, Fundação Ezequiel Dias, Belo Horizonte, MG, Brazil
[e] Serviço de Virologia e Riquetsioses, Diretoria do Instituto Octávio Magalhães, Fundação Ezequiel Dias, Belo Horizonte, MG, Brazil

ARTICLE INFO

Keywords:
SARS-CoV-2
Inactivated virus
RT-qPCR
ELISA
$PRNT_{50}$

ABSTRACT

Viral inactivation for antibody induction purposes, among other applications, should ensure biosafety, completely avoiding the risk of infectivity, and preserving viral immunogenicity. β-propiolactone (BPL) is one of the most used reagents for viral inactivation, despite its high toxicity and recent difficulties related to importation, experienced in Brazil during the SARS-CoV-2 pandemic. In this context, the main objectives of this work were to test different inactivation procedures for SARS-CoV-2 and to evaluate the induction of neutralizing antibodies in mice immunized with antigenic preparations obtained after viral treatment with formaldehyde (FDE), glutaraldehyde (GDE), peroxide hydrogen (H_2O_2), as well as with viral proteins extract (VPE), in parallel with BPL. Verification of viral inactivation was performed by subsequent incubations of the inactivated virus in Vero cells, followed by cytopathic effect and lysis plaques observation, as well as by quantification of RNA load using reverse transcription–quantitative real time polymerase chain reaction. Once viral inactivation was confirmed, cell culture supernatants were concentrated and purified. In addition, an aliquot inactivated by BPL was also subjected to viral protein extraction (VPE). The different antigens were prepared using a previously developed microemulsion as adjuvant, and were administered in a four-dose immunization protocol. Antibody production was comparatively evaluated by ELISA and Plaque Reduction Neutralization Tests (PRNT). All immunogens evaluated showed some level of IgG anti-SARS-CoV-2 antibodies in the ELISA assay, with the highest levels presented by the group immunized with FDE-inactivated viral antigen. In the PRNT results, except for VPE-antigen, all other immunogens evaluated induced some level of neutralizing anti-SARS-CoV-2 antibodies, and the FDE-antigen stood out again with the most expressive values. Taken together, the present work shows that FDE can be an efficient and affordable alternative to BPL for the production of inactivated SARS-CoV-2 viral antigen.

1. Introduction

Severe acute respiratory syndrome coronavirus 2 (SARS-CoV-2) has emerged in December of 2019 in Hubei Province of China and rapidly spread around the world, causing a global pandemic of coronavirus disease 19 (COVID-19) that is still ongoing (Wang et al., 2021). Infection by SARS-CoV-2 can be asymptomatic, present mild to moderate cold-like manifestations or can progress to acute respiratory distress syndrome, coagulation disorders and a range of other symptoms that ultimately may lead to death (Tsai et al., 2021). Due to the remarkable infectivity of SARS-CoV-2, mass vaccination is shown to be the main prophylactic strategy to contain the pandemic (Dai and Gao, 2021). However, there are groups of immunosuppressed individuals unresponsive to active vaccination, such that viral neutralization by passive immunization through transferred antibodies (Ledford, 2021), monoclonal preparations (Suryadevara et al., 2021), hyperimmune heterologous plasma (Pan et al., 2020; da Costa Camila et al., 2021; Vanhove et al., 2021), or plasma from convalescent donors (Piechotta et al., 2020; Chai et al.,

* Corresponding author.
E-mail address: sergio.caldas@funed.mg.gov.br (S. Caldas).

https://doi.org/10.1016/j.molimm.2022.05.012
Received 15 December 2021; Received in revised form 16 May 2022; Accepted 18 May 2022
Available online 23 May 2022

2020; Focosi and Franchini, 2021) have been seen as a rational complementary therapeutic approach. To address both the induction of antibodies for passive immunization and vaccination, the use of chemically inactivated virus is a traditionally used alternative (Delrue et al., 2009; Furuya, 2012).

Viral inactivation for antibody induction purposes must be concerned with safety, completely preventing virus infectivity; and with preserving viral immunogenicity, to induce a robust immune response. The optimal conditions for viral inactivation can vary with virus type, strain, concentration, incubation time, among other variables, implying that the procedure must be carefully defined to achieve a functional product (Delrue et al., 2012; Herrera-Rodriguez et al., 2019).

β-propiolactone (BPL) is one of the most widely used agents for viral inactivation and has traditionally been used in several vaccine preparations (Sabbaghi et al., 2019), including Corona Vac/Sinovac Biotech (formerly picovacc), one of the first authorized COVID-19 vaccines for "emergency use" in Brazil, China, and Indonesia (Gao et al., 2020; Fortner and Schumacher, 2021). However, in the rush of a race to obtain vaccines and therapeutics to fight COVID-19, the supply of BPL was compromised in some countries, including Brazil, and its price was inflated to even more prohibitive values, especially for countries in development.

On the other hand, fixation of infectious samples using formaldehyde (FDE) is a well-established protocol in electron microscopy for transforming active viruses into a non-infectious but structurally intact form in order to allow a proper diagnosis based on morphology (Möller et al., 2015). Although not unanimous for all viruses, many FDE-inactivated vaccines work well and protect against disease in the challenge (Bell et al., 1994; Furesz et al., 1995; Choi et al., 2003; Samina et al., 2005; Kistner et al., 2007; Heinz et al., 2008).

Cellular ultrastructure preservation by glutaraldehyde (GDE) is also well documented since the 1960s (Sabatini et al., 1963). GDE has been used in different assays dependent on morphological and/or antigenic preservation, such as chromatin isolation and electron microscopy in cancer cells (Sabatini et al., 1963; Chu et al., 2011), detection of specific mRNA molecules alongside morphologic preservation (Cubas-Nuñez et al., 2017), and inactivation of different viruses, including for vaccine purposes (Graham and Beveridge, 1990; Rodgers et al., 1985; Keles et al., 1998).

Inactivation of microbes with hydrogen peroxide (H_2O_2), as with other oxidizing agents such as nitric oxide and superoxide, represents a key element of the mammalian innate immune system to inactivate intracellular pathogens (Valko et al., 2007). Amanna et al. (2012), proposed the use of H_2O_2 as a possible viral inactivation platform for vaccine production. According to the authors, H_2O_2 rapidly inactivates viral nucleic acids with minimal interference with their antigenic structures or immunogenicities and it is a highly effective method when compared to conventional vaccine inactivation approaches, including FDE and BPL.

In terms of toxicity, BPL and FDE are currently regulated by OSHA as carcinogens. With the exception of BPL, all those previously mentioned reagents include the health effect (HE) code HE-14 (Marked irritation: Eyes, Nose, Throat, Skin); and symptoms such as skin irritation, blistering, burns, as well as corneal opacity, dysuria and hematuria (blood in the urine) are also described for BPL (source: Occupational Safety and Health Administration (OSHA) available at https://www.osha.gov/chemicaldata). Despite the evident toxicity, the concentrations of those reagents used in the processes and studies of viral inactivation for antigenic purposes are very low, being practically null after the concentration/purification of the final products.

According to Rodgers et al. (1985), other inactivation procedures, such as the application of heat, alcohol, or radiation, can impair the structural characteristics of viruses, not being suitable for applications that require such viral preservation. Nevertheless, Gamma irradiation can also be used to inactivate viruses, although multiple influencing factors must be considered, such as solute protein content, virus concentration, temperature and the volume of air, possibly related to the amount of oxygen free radicals produced in the reaction (Elliott et al., 1982; Hume et al., 2016; Elveborg et al., 2022). Furthermore, considering that SARS-CoV-2 is classified as a Risk Group 3 biological agent, high-titer virus stocks require biosafety level 3 (BSL-3) facilities for its handling (Yeh et al., 2021) but gamma irradiators are not located within these laboratories due to a multitude of practical reasons (Hume et al., 2016). Other operational disadvantages of using gamma irradiation include the need to work with radioactive materials and to remain in compliance with the increasing regulatory requirements naturally desirable to minimize health and environmental risks (IAEA, 2016). In this sense, there are still some concerns regarding biosafety, reduced antigenicity and the fact that the equipment is too bulky and expensive for some settings (Elveborg et al., 2022).

In view of this scenario, this work sought to investigate whether low-cost and easily obtainable chemical agents, such as FDE, GDE and H_2O_2 could be an alternative to BPL for inactivating SARS-CoV-2, while preserving the ability of the viral antigen to induce neutralizing antibodies in mice.

2. Materials and methods

2.1. Animals and cells

Twenty-eight Swiss Webster mice aged 21–28 days were obtained from the breeding facility of Fundação Ezequiel Dias (FUNED). Animals were randomly divided into seven groups of four mice and kept in individually ventilated cages (Ventilife policarbonate Mini-Insulator, Alesco®). Experimental groups were kept under controlled temperature (20–24 °C), lighting cycles of 12 h and food and water available ad libitum. All experimental procedures involving mice were carried out in accordance with the Ethical Principles of Animal Experimentation, adopted by the Ethics Committee on the Use of Animals (CEUA/FUNED Number 010/2020).

Vero E6 and Vero CCL-81 cells were maintained at 37 °C with 5% CO_2 in Minimum Essential Medium (MEM) (Gibco) supplemented with 5% fetal bovine serum (FBS) (Gibco), 100 μg/mL of streptomycin, and 100 IU/mL of penicillin (LGC Biotecnologia).

2.2. Virus culture

2.2.1. Virus isolation

All experiments with active SARS-CoV-2 were performed in biosafety level 3 laboratory (BSL-3) by personnel equipped with powered air-purifying respirator. The virus was isolated from a sample submitted to molecular diagnosis by FUNED (approved by the Research Ethics Committee with CAAE Number 32850420.4.0000.9507) the public central laboratory responsible for the diagnosis of COVID-19 in the state of Minas Gerais, Brazil. The viral genome was identified as lineage B.1.1.28 (GISAID access number EPI_ISL_11454762) using the Ion Torrent Sequencing Platform and the Genome Detective tool (https://www.genomedetective.com/). The second and third passages in Vero E6 cells were used as a seed pool for virus multiplication.

2.2.2. Virus multiplication

Confluent monolayers of Vero E6 cells were inoculated with SARS-CoV-2 at a multiplicity of infection (MOI) of 0.001 in 175 cm^2 flasks. After adsorption for 1 h at 37 °C, MEM supplemented with 2% FBS and antibiotics, was added. Monolayers of non-infected cells were run in parallel. Culture supernatants were collected and clarified by centrifugation on the third day of infection and were maintained at −70 °C.

2.2.3. Virus titration

Virus titration was carried out in 12-well plates seeded with VERO CCL-81 cells at a concentration of 1×10^5 cells/well. Supernatant dilutions, ranging from 10^{-1} to 10^{-5} in MEM without FBS, were

transferred (250 μL/well), in duplicates, to the seeded plates. After adsorption, an overlay of 1.5% of carboxymethylcellulose (CMC) (Sigma-Aldrich) with MEM, 1% FBS, 100 μg/mL of streptomycin, and 100 IU/mL of penicillin was added to the wells, and plates were incubated for 72 h at 37 °C in 5% CO_2. Then, plates were fixed with 10% formaldehyde for 1 h, stained with 1% crystal violet (Synth) solution for 5 min and washed. To determine viral titer as Plaque Forming Units (PFU)/mL, lysis plaques were counted, and the values were plotted.

2.3. Virus inactivation

A single viral suspension was divided into 50 mL aliquots for treatment with different inactivating agents diluted in MEM medium. β-propiolactone (BPL) 98.5% (Natalex S.A.) was used at a 1:8000 dilution, and the formaldehyde (FDE) 37.5% (Química Moderna), glutaraldehyde (GDE) 8% (Sigma-Aldrich) and hydrogen peroxide (H_2O_2) 50% (Sigma-Aldrich) reagents were used at the 1:1000 dilution. Viral suspensions were incubated for 24 h at room temperature for the inactivation procedure, being stored at −70 °C until confirmation of virus inactivation. As a negative control, an untreated aliquot of SARS-CoV-2 suspension was incubated at the same conditions.

2.4. Confirmation of viral inactivation

2.4.1. Determination of residual virus infectivity in cells

To prove viral inactivation and/or verify the presence of residual active virus, were adsorbed in quadruplicates, for 1 h at 37 °C in 12-well plates monolayers of Vero CCL-81 cells, one, two or three non-cytotoxic log dilutions of each inactivated viral suspension. Here it was necessary to use dilutions ranging from 10^{-1} to 10^{-3} depending on the chemical reagent, in order to eliminate specific cytotoxic effect interferences of each reagent. As a negative control for each inactivation check assay, we used the same dilution of non-inactivated virus. Then, supernatants were replaced by semi-solid medium and, after incubation for 72 h at 37 °C, plates were fixed with 10% formaldehyde and stained with 1% crystal violet solution, as described in the viral titration session.

In addition, an alternative strategy was also used to confront the viral inactivation results observed in the previous verification test. Flasks of 25 cm^2 containing 1 × 10^6 Vero E6 cells were inoculated with non-cytotoxic dilutions of virus inactivated by the different used protocols. After 1 h of adsorption, the inoculum was removed, and monolayers were washed with phosphate buffered saline (PBS). MEM medium with 2% FBS was added and the flasks were incubated for up to seven days. A flask with untreated cells was included as a negative control to check a possible cytopathic effect (CPE) caused by any residual cytotoxicity associated with the reagents used in the test. Likewise, an active SARS-CoV-2-infected control was included. After incubation for three and seven days, cell cultures were checked for CPE and compared with SARS-CoV-2-infected control at the same dilutions. Then, viral genetic material content of inactivated viral samples was evaluated by reverse transcription–quantitative real time polymerase chain reaction (RT–qPCR). Samples from each flask kept for seven days were retested in a plate lysis assay for further confirmation of viral inactivation.

2.4.2. RT-qPCR

Viral RNA was extracted using QIAmp® Viral RNA Mini Kit (Qiagen). Reverse transcription and polymerase chain reaction were performed in a single step using the GoTaq® Probe 1-Step RT-qPCR System kit (Promega). The primers and probe used, as described for the SARS-CoV-2 diagnostic protocol carried out by the CDC (https://www.cdc.gov/coronavirus/2019-ncov/lab/rt-pcr-panel-primer-probes.html). The extracted RNA from each sample (2 μL) was added to 8 μL of the reaction mixture. Thermocycling consisted of an initial stage of reverse transcription at 50 °C for 30 min, followed by an initial DNA polymerase activation at 95 °C for 5 min and 40 amplification cycles at 95 °C for 15 s and 55 °C for 1 min, with fluorescence acquisition at 55 °C.

2.4.2.1. Molecular quantification strategy. The molecular quantification strategy performed consisted firstly in determining the amplification efficiency of the oligonucleotides set used. For this purpose, a four-log dilution was performed from a viral sample which had its viral titer in PFU/mL determined, according to the methodology previously described. The efficiency (E) of amplification was determined automatically by the StepOne™ Software v2.0 by calculating: $E = 10^{(-1/slope)}$-1. Viral RNA loads were quantified using the comparative Ct method relative to a reference (ref) sample of known viral titer. Thus, the relative values were converted to PFU/mL equivalents using the following calculations: $(1 + n)^{-(\Delta Ct \pm \Delta CtSd)}$, where n corresponds to amplification efficiency; Ct (threshold cycle) is the intersection between amplification curve and the threshold line; $\Delta Ct = (Ct_{sample\ mean} - Ct_{ref\ mean})$; $\Delta CtSd = \sqrt{Sdsample^2 + Sdref^2}$ and Sd = Standard deviation.

The inactivation treatment was considered successful when no lysis plaque and CPE were observed in any replicate, in addition to drops in RNA load greater than three logs in both analyzes performed three and seven days after virus incubation in cell cultures.

2.5. Viral concentration and purification

This process was adapted from Dent and Neuman (2015). Aliquots of 50 mL from cell culture supernatants containing 1.3 × 10^7 PFU/mL of inactivated SARS-CoV-2 and non-infected cell culture supernatant (mock) were prepared and filtered over a 0.22 μm sterilizing grade filtering unit. Polyethylene glycol 8000 (PEG 8000) (8%) (Sigma-Aldrich) and sodium chloride (NaCl) 2.2% (Fisher Scientific) were added to the supernatants and kept overnight at 4 °C, under constant stirring. Afterwards, the viral suspension was centrifuged at 10,000 x *g* at 4 °C for 10 min. After centrifugation, the pellet was resuspended in 1 mL of sterile TES buffer (0.01 M Tris; 0.15 M NaCl; 0.001 M EDTA; pH 7.2) at 4 °C and purified in a discontinuous sucrose gradient. For this, solutions of 10%, 20% and 30% sucrose (Vetec) were prepared in TES buffer and 1.5 mL of each solution were gradually (from the highest concentration to the lowest) added to 16 × 76 mm polystyrene tubes. The concentrated viral suspensions were gently added to the tube to form a visible and opaque phase on top of the sucrose solutions. The tubes were subjected to ultracentrifugation (Beckman J2-MC centrifuge; JA-21 rotor) at 54,000 x *g* for 3 h at 4 °C. The pellet was resuspended in 550 μL of cold PBS, aliquoted, and immediately stored at −70 °C. Protein content of purified virus samples was determined by fluorometric quantification on QUBIT® spectrophotometer, with the Qubit® Protein Assay Kit (Invitrogen).

2.6. Protein extraction from BPL-inactivated virus

After viral purification, one sample inactivated by BPL was subjected to protein extraction, using the NucleoSpin® TriPrep DNA, RNA, and protein purification kit (Macherey-Nagel), in order to obtain a BPL-inactivated SARS-CoV-2 protein suspension, devoid of viral structure.

2.7. Polyacrylamide gel electrophoresis

Protein separation of the inactivated SARS-CoV-2 samples occurred through one-dimensional electrophoresis in a 10% sodium dodecyl-sulfate polyacrylamide gel electrophoresis (10% SDS-PAGE). Proteins were diluted in non-denaturing buffer and heated to 95 °C for 5 min. BLUeye Prestained Protein Ladder (Sigma-Aldrich) with a molecular weight range of 20–245 kDa was applied in parallel to estimate protein masses of the antigen samples. Electrophoresis took place in an appropriate vat containing glycine buffer and SDS, connected to a power source at 100 V, 300 mA, 40 W for 45–60 min. Protein staining was done with Coomassie Blue dye.

2.8. Mice immunization

To assess the immunogenic potential of the virus inactivated by the different methodologies, the humoral immune response elicited by these antigens was evaluated in mice. Six groups of four animals were formed, which were immunized using the antigens obtained with different inactivating agents (BPL, FDE, GDE and H_2O_2), and with the VPE, in addition to the mock control group, all of them incorporated in the adjuvant. A microemulsion formulation was used as adjuvant for the immunization and it was prepared under sterile conditions, according to the procedure previously developed by Leclercq et al. (2011). For its preparation a single emulsion containing polysorbate 80, isopropyl myristate and water in the proportion of 6:1:9 v/v, respectively, was firstly obtained using an UltraTurrax equipment set at the rate of 8000 rpm for 20 min. Next, one volume of propylene glycol was added to the formed emulsion and homogenized at 8000 rpm for 20 min until formation of the microemulsion. Prior to the immunization, aliquots of 124 μL, corresponding to approximately 50 μg of protein for each sample, were mixed with 320 μL of the microemulsion. Four immunization doses were given per animal, with an interval of 15 days between the first two doses, 10 days between the second and the third doses and seven days between the third and the last doses. After each dose, approximately 120 μL of blood was collected by retro-orbital vein puncture in tubes containing EDTA (Promega) at 18 mg/mL and pH 6.6–6.8 corresponding to about 10% of the collected blood volume. During the immunization schedule, animals were weighted and monitored to assess possible signs of antigen toxicity. Afterwards, mice were euthanized by overdose of xylazine (30 mg/kg) (Syntec) and ketamine (240 mg/kg) (Venco) and cardiac puncture was performed for total blood collection, under anticoagulant conditions. Samples were centrifuged at 952 x g for 10 min and the obtained plasma was kept at −20 °C until use.

2.9. ELISA

To evaluate antibody production in immunized animals, indirect ELISA was performed. Polystyrene 96-well plates were coated overnight at 4 °C with 100 μL of a solution containing 10^4 PFU/mL of BPL-inactivated SARS-CoV-2 diluted in carbonate buffer pH 9.6. Wells were rinsed with PBS-Tween 0.05% and blocked with a 2% solution of bovine serum albumin (BSA) (Sigma-Aldrich) for 1 h at 37 °C. After blocking, plates were incubated with mice plasma diluted in PBS (1:100) at 37 °C for 1 h and 30 min. Plates were then washed three times with PBS-Tween and incubated again at 37 °C for 1 h with HRP-conjugated goat anti-mouse IgG (Sigma-Aldrich) diluted 1:1000. Plates were washed again three times and incubated with hydrogen peroxide substrate-chromogen solution and TMB (3,3′,5,5′-tetramethylbenzidine) substrate (BD OptEIA) at 37 °C for 30 min. The reaction was stopped by the addition of 2 M sulfuric acid and the absorbance was measured at 450 nm.

2.10. Plaque reduction neutralization test (PRNT)

To assess the neutralizing potential of the antibodies elicited by the different immunogens, a plaque reduction assay was performed. The assay was conducted in duplicates, using 12-well tissue culture plates containing 1×10^5 Vero CCL-81 cells/well. Serial dilutions of each immunized mice plasma sample were incubated with 30–100 SARS-CoV-2 PFU for 1 h at 37 °C. The virus-serum mixtures were added onto pre-formed cell monolayers and incubated for 1 h at 37 °C in 5% CO_2. The cell monolayer was then overlaid with CMC 1% plus MEM supplemented with 1% FBS, 100 μg/mL of streptomycin, and 100 IU/mL of penicillin, and the plates were incubated for three days at 37 °C in 5% CO_2. Then, plates were fixed and stained as mentioned above. Antibody titers were defined as the highest serum dilution that resulted in reduction of >50% ($PRNT_{50}$) in the number of virus plaques. This method has been extensively validated for SARS-CoV-2 previously (Perera et al., 2020).

2.11. Statistical analysis

Data normality was verified by the Shapiro-Wilk test ($P > 0.05$). One-way ANOVA and Tukey's multiple post-test comparisons were performed for each time, when applicable. For the PRNT analysis, the data were lognormal transformed. For the analysis of viral RNA load, comparisons between treated and untreated groups were performed using the non-parametric Mann Whitney test.

3. Results

After multiplication in Vero E6 cells, the SARS-CoV-2 isolate (lineage B.1.1.28), was submitted to viral titration, presenting 1.3×10^7 PFU/mL. The viral RNA quantification strategy used in this study proved to be adequate and easy to perform for the molecular quantification of SARS-CoV-2 subjected to different inactivation procedures. Fig. 1 shows the amplification plot (Fig. 1A) and its corresponding standard curve (Fig. 1B) generated from five log dilutions of a standard sample equivalent to 1×10^7 PFU/mL. The amplification efficiency determined was about 90% ($R^2 = 1$) and this value was used for viral quantification by the comparative Ct method.

After defining the molecular quantification strategy, we started the viral inactivation procedures. Fifty milliliters aliquots of the SARS-CoV-2 isolate viral suspension were treated for 24 h at room temperature with four different inactivating reagents. The success of the inactivation procedures was confirmed through incubations of the treated samples with cell cultures, where no CPE suggestive of multiplication of residual active virus or plaque formation were observed. Only the active control viral sample showed cytopathic effect and plaque formation. Fig. 2 shows the characteristic cytopathic effects observed after incubation of cells with active virus (Fig. 2A) compared to non-infected cells (Fig. 2B) and cell lysis plaques triggered by viral infection at different dilutions (Fig. 2C).

There were no significant differences for the levels of residual RNA among different viral treatments, although a slight tendency to reduce the viral RNA load was observed in all of them when comparing the third to the seventh day of incubation in cell culture. While in the active virus control groups, for the four viral inactivation assays, a significant increase in viral RNA levels was observed when comparing the third to the seventh day of viral incubation. In general, the reduction in viral RNA load of the different treatments, in relation to the respective control groups, was always greater than three logs, ranging from about 3.5–4.5 logs for the analyzes after three days of incubation and about 4.5–5 logs for analyzes on day seven of incubation (Fig. 3).

The viral antigens obtained after concentration and purification of SARS-CoV-2 inactivated by different chemical reagents evaluated in this study were submitted to 10% SDS-PAGE and a similar pattern of protein bands, many of them suggestive of coronaviruses, could be evidenced for all treated viruses (Fig. 4). SDS-PAGE was performed with a similar volume of purified viral product, and the different band intensities observed may indicate degradations or differential yields during processing. However, the objective of such SDS-PAGE was to observe if the pattern of the bands generated after the sucrose gradient purification would be the same for the different treatments. The similar pattern observed suggested that the virus was adequately recovered in the purification process employed.

Once the viral antigens were produced, mice were inoculated and monitored for weight loss and clinical signs during the immunization schedule. No apparent toxicity was observed in any experimental group, and the body weight curves did not show statistical differences ($P > 0.05$) in relation to the mock-control group (Fig. 5).

The ELISA assay performed two weeks after the first immunization (day 15) showed detectable levels of anti-SARS-CoV-2 antibodies in all

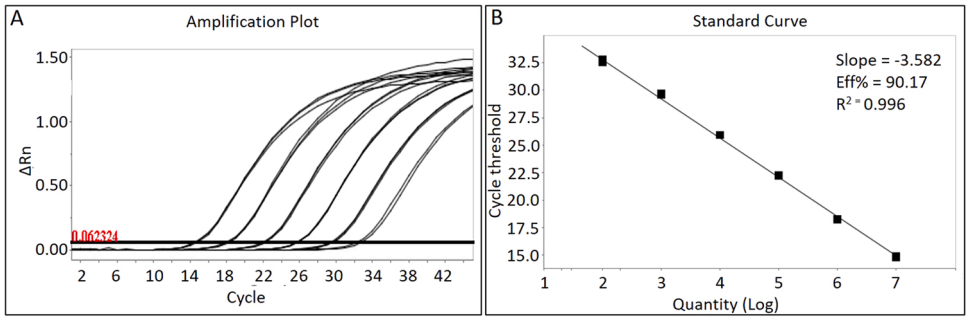

Fig. 1. Determination of amplification efficiency for the molecular quantification of SARS-CoV-2 by the comparative Ct method. (A) Amplification curves generated with four log dilutions of a viral RNA sample equivalent to the initial titer of 1×10^7 PFU/mL. (B) Standard curve generated from the linear region of each amplification curve. Efficiency of amplification was determined using the equation: efficiency (E) $= 10^{(-1/\text{slope})}$-1, being E = 90.17% and $R^2 = 0.996$.

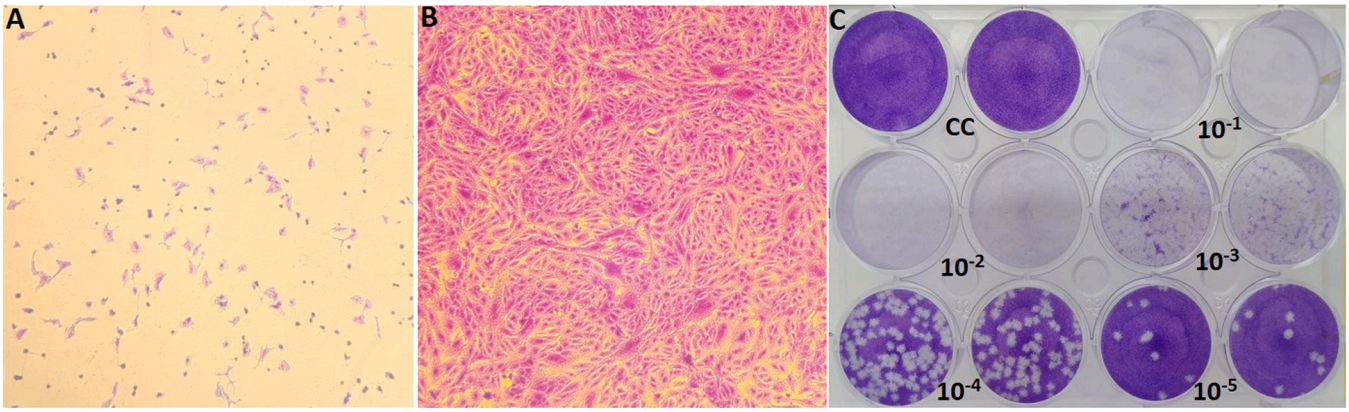

Fig. 2. Typical cytopathic effect and lysis plaques induced by SARS-CoV-2 infection in Vero cells. (A) Cytopathic effect observed under a light microscope (100X magnification) in Vero E6 cells infected with SARS-CoV-2, (B) compared to non-infected cells, and (C) cell lysis plaques observed after incubation of different viral dilutions (10^{-1} to 10^{-5}) in Vero CCL-81 cells, compared to non-infected control cells (CC) in 12-well plate assay.

groups of mice immunized with the different immunogens evaluated. At 10 days after the second immunization (day 25), the highest antibody levels were induced equally in the groups immunized with FDE- and BPL-antigens. Mice immunized with GDE-antigens showed intermediate levels while the lowest levels were observed in the groups that received H_2O_2- and VPE- antigens (Fig. 6).

At seven days after the third immunization (day 32), FDE-antigen group showed higher levels of antibodies, while no increase in antibodies levels was observed in the group with VPE-antigen. The same was observed in the last analyzed performed three days after the fourth immunization (day 35). The groups immunized with H_2O_2-, BPL- and GDE-antigens showed intermediate similar levels (Fig. 6).

We observed that plasma from the group of mice immunized with FDE-inactivated SARS-CoV-2 antigen showed the highest neutralizing antibody titer. When the four animals of FDE-group were pooled, the neutralizing antibody titer was 1:1856, ranging from 1:1615 to 1:2463 in the individual analyses. The GDE-group showed a pooled titer of 1:1076, ranging from 1:289–1:1818 for mice individually. The BPL-group showed a titer of 1:640 when pooled, ranging individually from 1:406–1:1267. However, no significant differences were observed between the GDE- and the BPL-group. The group immunized with H_2O_2-antigen showed no expressive titers of neutralization when compared to the other groups. The plasma pool of H_2O_2-antigen group was 1:320 and the individual mice plasmas showed titers ranging from 1:20–1:92. The group of mice immunized with VPE-antigen did not show neutralizing titers even when pooled (Fig. 7).

4. Discussion

In this study, we sought to evaluate different SARS-CoV-2 chemical inactivation strategies potentially as effective as BPL in inactivating SARS-CoV-2, without critically compromising its antigenicity in terms of producing neutralizing antibodies. The successful inactivation of the virus allows its transfer from a BSL3 to a BSL2 laboratory environment, which can reduce the risk of accidental infections due to unsafe laboratory practices. In addition, the new coronavirus pandemic has driven the development of different strategies to combat COVID-19, in the area of diagnosis, vaccines and treatments. An example, developed by our group, is the experimental production of anti-SARS-CoV-2 hyperimmune polyclonal antibodies from the immunization of horses with the whole virus inactivated with BPL. However, in our study great difficulties were faced to obtain the BPL for experimental purposes, which was prohibited from being imported into Brazil by air, and the product suppliers in the country did not offer the sale by sea import. In this sense, aiming at evaluating alternatives for viral inactivation, we decided to test the potential of inducing neutralizing antibodies in mice, from SARS-CoV-2 inactivated with different chemical reagents. Thus, parallel to the BPL, we tested the FDE, GDE and H_2O_2 chemical reagents as well as the VPE obtained with the virus traditionally inactivated with BPL, using mock as control. The same batch of virus was used for all antigen preparations in order to compare the potential of each of them to induce a neutralizing immune response against SARS-CoV-2.

The BPL viral inactivation protocol was based on two studies with SARS-CoV (Lu et al., 2005; Roberts et al., 2010), in addition to the institutional procedure for the production of heterologous hyperimmune anti-rabies serum at Funed. Our results showed that BLP at a

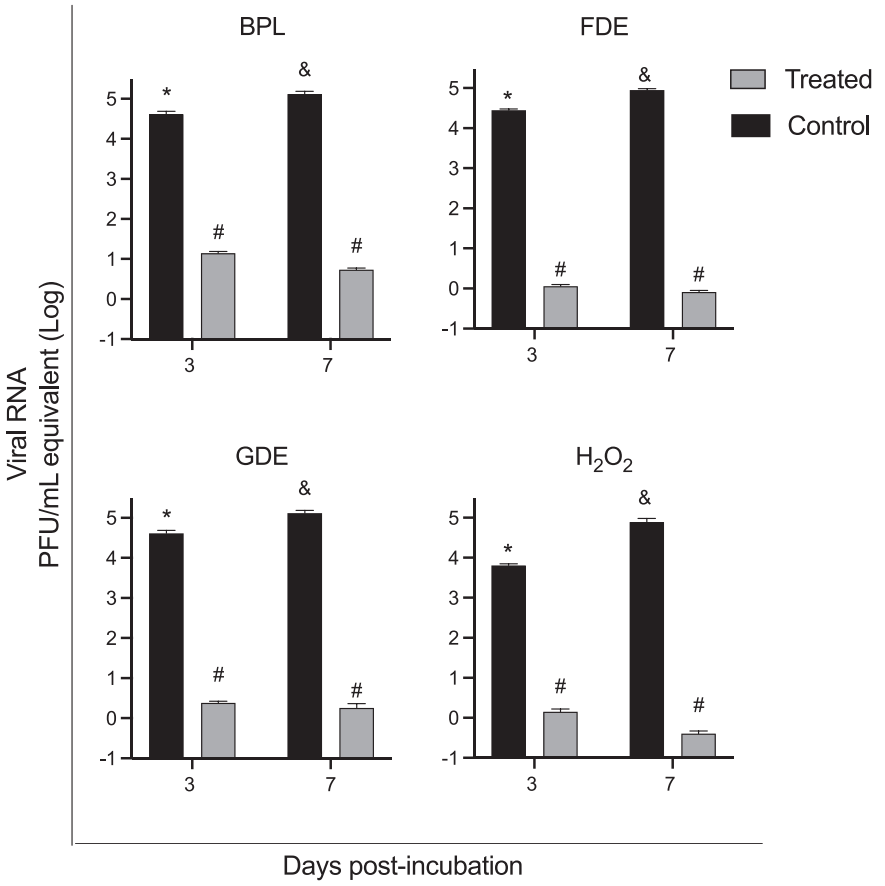

Fig. 3. Quantification of viral RNA in supernatant from Vero E6 cells challenged with inactivated viral suspensions. The supernatants were collected on days three and seven post-challenge. Gray columns indicate virus inactivated by β-propiolactone (BPL), formaldehyde (FDE), glutaraldehyde (GDE) and hydrogen peroxide (H_2O_2), and black columns represent untreated viral controls. Different symbols indicate significant difference ($P > 0.05$).

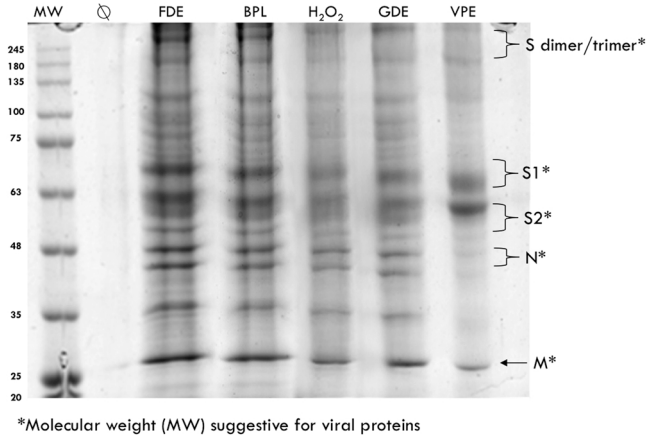

Fig. 4. 10% sodium dodecyl-sulfate polyacrylamide gel electrophoresis of SARS-CoV-2 inactivated with formaldehyde (FDE), β-propiolactone (BPL), hydrogen peroxide (H_2O_2), glutaraldehyde (GDE) and virus proteins extracted (VPE). The protein bands were stained with coomassie blue dye.

1:8000 dilution was suitable for the complete inactivation of SARS-CoV-2 in a 24 h treatment at room temperature. The mechanism of BPL viral inactivation seems to be related to its interaction with purine bases, with consequent breakdown of the nucleic acid structure, and with protein interactions, affecting their conformation and dynamics, as well as inducing changes in the surface of viral capsids (Uittenbogaard et al., 2011; Delrue et al., 2012; Fan et al., 2017).

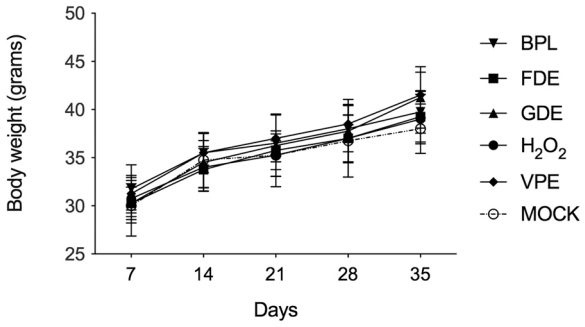

Fig. 5. Body weight of mice inoculated with different preparations of SARS-CoV-2 antigens. Mean body weight monitored over the tests performed with groups of mice inoculated with antigenic preparations of SARS-CoV-2 inactivated with β-propiolactone (BPL), glutaraldehyde (GDE), formaldehyde (FDE), hydrogen peroxide (H_2O_2), virus proteins extracted (VPE), and control inoculated with non-infected cell supernatant (Mock). No significant difference was observed in any of the experimental groups evaluated ($P > 0.05$).

The choice of 1:1000 dilutions for FDE 37% and GDE 8% were based on the study by Darnell et al. (2004), which demonstrated the inactivation of SARS-CoV using different methodologies. FDE-mediated viral inactivation appears to occur from its binding with nonprotonated amino groups, such as lysine, generating hydroxymethylamine. The hydroxymethylamine in turn combines with amino, amide, guanidyl, phenolic or imidazole groups to create inter- or intramolecular methylene cross-links (Darnell et al., 2004; Jiang and Schwendeman, 2000). FDE can also act by blocking the genome reading through the alkylation

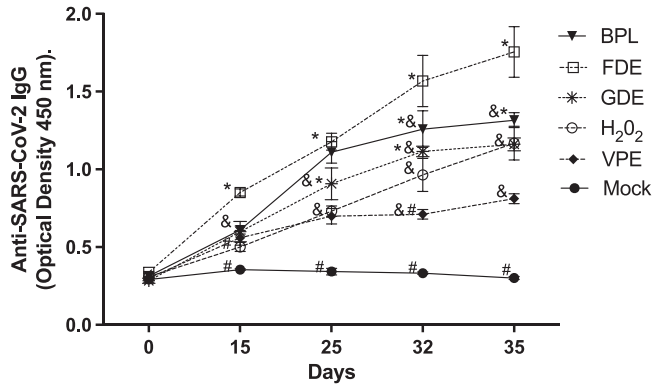

Fig. 6. IgG levels detected by ELISA in the plasma of mice immunized with SARS-CoV-2 antigens. The mice groups received a schedule of four immunizations with SARS-CoV-2 inactivated with β-propiolactone (BPL), glutaraldehyde (GDE), formaldehyde (FDE), hydrogen peroxide (H_2O_2), viral protein extract (VPE) and non-infected cell culture supernatant (Mock). Different symbols indicate significant difference ($P > 0.05$).

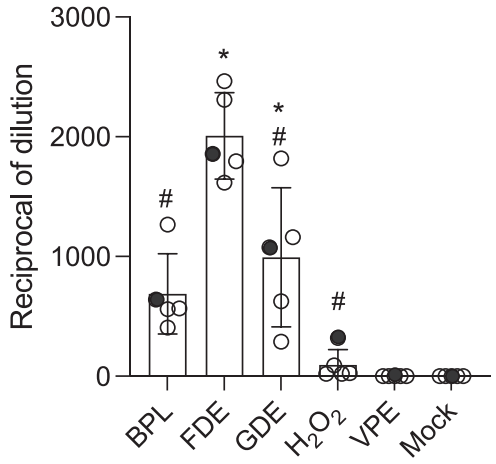

Fig. 7. Plaque reduction neutralization test (PRNT) performed with plasma from mice immunized with SARS-CoV-2 antigens. Mice groups received a schedule of four immunizations with SARS-CoV-2 inactivated with β-propiolactone (BPL), formaldehyde (FDE), glutaraldehyde (GDE), hydrogen peroxide (H_2O_2), viral protein extract (VPE) and non-infected cell culture supernatant (Mock). Data are expressed as reciprocal of dilution equivalent to $PRNT_{50}$. In each column, the open circles correspond to the $PRNT_{50}$ observed for the animals tested individually, while the closed circles correspond to the $PRNT_{50}$ observed with the pool of the four animals of each group. Different symbols indicate significant difference ($P > 0.05$).

of the adenine nucleotide in DNA and/or RNA molecules. In a similar way, GDE appears to act on both proteins and genomic DNA or RNA, since alike chemical groups are present in both compounds, and RNA and protein synthesis can be blocked by this aldehyde (Darnell et al., 2004; Delrue et al., 2012).

Finally, the choice of H_2O_2 was based on the work of Amanna et al. (2012), which introduced a new H_2O_2-based vaccine platform for viral inactivation. In our preliminary tests we found the 1:1000 dilution of 50% H_2O_2 to be adequate for inactivating SARS-CoV-2 for 24 h at room temperature. The viral inactivation mechanism of H_2O_2 appears to be related to genomic damage caused by hydroxyl radicals, which attack carbon double bonds and result in the breakdown of viral genetic material and loss of viability (Amanna et al., 2012).

In our work, we observed complete inactivation by all chemical reagents under the established conditions with confirmation of inactivation by plaque assays and challenge on permissive cells in culture bottles. The last one was a method adapted to verify the virus outgrowth, which is highly sensitive because it allows verify the outgrowth of as little as a single infectious unit. This is confirmed by observing the cytopathic effect formation after seven days of incubation, compared to cell and virus controls, together with RT-qPCR assay of the cells supernatant that were challenged with the inactivated inoculum.

It is worth noting that the genomic and even the subgenomic RNAs of SARS-CoV-2 cannot be considered an indicator of active replication. At least a part of these RNAs is encapsulated in extracellular or double membrane vesicles, being protected from degradation by nucleases, even after replication has ceased (Alexandersen et al., 2020). For this reason, we adopted the strategy of repeating RNA quantifications after three and seven days of infection, compared to the untreated control. The absence of viral replication could be evidenced by the maintenance of residual RNA levels, in the case of viral inactivation, while for the active virus, an increase in viral RNA levels was observed.

In this sense, the viral RNA quantification strategy used to confront CPE and cell viability data added robustness to our proof of viral inactivation. The abrupt drop in viral RNA, remaining stable on days three and seven, strongly evidenced viral inactivation when compared to the active virus control, which maintained high RNA levels during the same period of evaluation and challenged dilutions. Furthermore, RT-qPCR data were suggestive of viral replication for the active virus controls when comparing the third- and seventh-day post inoculation, whereas no evidence of replication was observed in the treated viruses.

It is also important to point out that the gold standard method to assess virus neutralization and/or inactivation is by checking the formation of lysis plaques in infected cell cultures. Here we performed one more additional check with re-inoculation of the material collected after the seven-day challenge in cell culture bottles. The non-observation of CPE and plaque formation in any of those cellular challenges was compatible with the results obtained in the above-mentioned qRT-PCR strategy, indicating success in the viral inactivations performed.

The viral antigens obtained after concentration and purification of SARS-CoV-2 inactivated by the different chemical reagents evaluated in this study were submitted to 10% SDS-PAGE and showed similar protein band profiles, suggesting homogeneity in the macrostructure of the viral proteins recovered after the different virus treatments, such as the suggestive molecular weight for the M protein of about 25 kda, the N-protein with about 46–58 kDa, the S2 subunit, which can be presented with 50.3–64.5 kDa, the subunit S1 around 67–85 kDa, as well as S-dimer around 180–200 kDa and S-trimer around 250 kDa (Bosch et al., 2003; Kuo et al., 2016; Ke et al., 2020; Li et al., 2021).

Once confirmed the viral inactivations and success in obtaining the viral antigen through RT-qPCR and SDS-PAGE analyses, we started the immunizations of mice. We used the traditional Swiss Webster (SW) mice for the convenience of having this outbred mouse strain in our institution with high production control. These animals are used in the DL-50 tests, as one of the quality controls for the release of our heterologous therapeutic sera produced here, in addition to many of our scientific research. Furthermore, SW mice are easy to acquire and manage, having been widely used for decades as an all-purpose stock for drug safety testing and scientific research (Le Nedelec and Rosengren, 2002; Costa et al., 2010; Tuttle et al., 2018). According to Tuttle et al., 2018, outbred mice may even show greater experimental replicability than inbred mice, due to a biological system that is less vulnerable to differences in environment and experimental conditions. At the same time, there is growing recognition that high-quality mouse stocks from heterogeneous origins provide a powerful experimental platform for a wide range of research applications, accounting for background genetic variations that are also naturally considered to other animals, including humans (Tuttle et al., 2018).

As an adjuvant, we used a microemulsion previously developed (Leclercq et al., 2011). However, unlike the previous work, the microemulsion was prepared without the antigen, which was mixed at the time of its administration. This modification aimed to make the use of

adjuvant microemulsion more accessible in different work infrastructures, such as the possible use for the immunization of horses in experimental farms deficient in a more complex laboratory structure. The monitoring of weights and clinical-behavioral manifestations of mice did not show apparent toxicity for any of the antigenic preparations, when compared to the control groups, showing that the chemical reagents and immunogen production method used were adequate. It is worth emphasizing that the concentration of the different reagents used for the viral inactivations were very low, (dilutions $>$ 1:1000), in addition to the fact that the viral concentration procedure itself recovers only the inactivated virus, eliminating all the supernatant with the chemical reagent used. Furthermore, even the assays to verify the viral inactivation before its purification, were carried out with the presence of chemical reagents in concentrations that did not demonstrate any cytotoxicity for the mammalian cells (Vero cells) used in the assays.

To broadly assess the consequences of different antigen preparations on antigenicity in relation to antibody production, we compared the antibody levels of the experimental groups by ELISA and PRNT. Although ELISA approach does not distinguish between neutralizing and non-neutralizing epitopes, this assay may indicate low or high levels of antibodies production against SARS-CoV-2. PRNT which measures neutralizing antibodies by in vitro virus neutralization is considered the best and most widely accepted approach to measuring protective antibodies (Roehrig et al., 2008; Perera et al., 2020).

In this work, the ELISA and PRNT analyzes suggested that FDE was the chemical reagent that best preserved the viral proteins, due to the highest induced anti-SARS-CoV-2 IgG titers, as well as the best $PRNT_{50}$ values. The mice immunized with VPE-antigen showed lowest levels of IgG and did not show neutralizing antibodies by PRNT. One of the hypothesis for the lack of stimulation of neutralizing antibodies may be related to protein linearization during the lysis and extraction process, compromising the induction of conformation-specific antibodies important for blocking the infection. In a somewhat similar way, the group of mice immunized with H_2O_2-antigen showed intermediate levels of IgG, when compared to FDE-antigen and the other antigens, but showed very low levels of neutralizing antibodies. The one reason may be that strong oxidizing agents from H_2O_2 irreversibly damage the basic molecular structure of proteins (Skykes, 1965).

Although some studies have reported that the inactivation of some viruses with FDE, as HIV (Rossio et al., 1998), canine parvovirus (Pollock and Carmichael, 1982) poliovirus (Tano et al., 2007) and porcine reproductive and respiratory syndrome virus (Delrue et al., 2009), could result in a loss of neutralizing response, in this work we observed high antibody titers against SARS-CoV-2 inactivated by FDE as well as BPL and GDE. Nevertheless, the virucidal effectiveness of FDE has been very well documented (Barteling and Woortmeyer, 1984; Salk and Gori, 1960) and several FDE-inactivated vaccines have shown adequate protection against disease on challenge, such as inactivated Ross River virus (RRV) (Kistner et al., 2007), West Nile virus (Samina et al., 2005), papilloma virus (Bell et al., 1994), Hantaan virus (Choi et al., 2003), hepatitis A virus (Furesz et al., 1995), tick-borne encephalitis virus (Heinz et al., 2008), among others.

In our study, the neutralizing capacity of the antibodies showed no statistical difference between GDE and BPL groups, but the group of mice immunized with FDE-antigen clearly showed the highest antibody levels and neutralizing power compared to the others. Thus, our data allow us to conclude that the FDE viral inactivation protocol used here is an efficient and affordable alternative to BPL for SARS-CoV-2 inactivation, overcoming the previously mentioned BPL acquisition difficulties. A practical application of these findings is that the antigenic material produced by this readily available chemical reagent appears to be able to preserve the conformation of viral epitopes for successful use in applications that require antigen-antibody interactions, such as the production of antigens for ELISA and indirect immunofluorescence reactions, as well as for the production of neutralizing polyclonal antibodies, among other applications.

Finally, it is noteworthy that although our results have suggested that FDE was the best reagent here evaluated for the antigenicity preservation of SARS-Cov-2 proteins, further studies are needed to confirm this hypothesis, including evaluation of cellular response and additional assays to confirm retention of epitope antigenicity.

CRediT authorship contribution statement

Emerson de Castro Barbosa: Conceptualization; Investigation; Writing – original draft**; Adriana de Souza Andrade:** Conceptualization; Investigation; Writing – original draft; **Myrian Morato Duarte:** Investigation; Writing – original draft; **Gilson Faria:** Investigation; Writing – original draft; **Felipe Campos de Melo Iani:** Investigation; Resources; Writing – original draft; **Ana Caroline Zampiroli Ataide:** Investigation; Writing – original draft; **Lucas Maciel Cunha:** Investigation; Formal analysis; Writing – original draft; **Clara Guerra Duarte:** Investigation; Writing – original draft; **Sílvia Ligorio Fialho:** Methodology; Resources; Writing – original draft; **Sérgio Caldas:** Conceptualization; Methodology; Investigation; Resources; Data curation; Writing – original draft; Writing – review & editing; Funding acquisition.

Funding

This work was supported by the Fundação de Amparo à Pesquisa do Estado de Minas Gerais, Brazil (APQ-00399–20) e Fundação Ezequiel Dias.

Declaration of Competing Interest

The authors declare that they have no conflict of interest.

Acknowledgements

We gratefully thank Karla de Santana Evangelista and Sophie Yvette Leclercq from Funed for their contributions in SDS-PAGE analyses; Ariadna Oliveira da Silva for her contributions to the preparation of the adjuvant microemulsion; Fernanda de Oliveira Silva and Luciene Silva de Souza Meira for their operational support in the laboratory routine where most of the tests for this work were performed.

References

Alexandersen, S., Chamings, A., Bhatta, T.R., 2020. SARS-CoV-2 genomic and subgenomic RNAs in diagnostic samples are not an indicator of active replication. Nat. Commun. 11, 6059. https://doi.org/10.1038/s41467-020-19883-7.

Amanna, I.J., Raué, H.P., Slifka, M.K., 2012. Development of a new hydrogen peroxide-based vaccine platform. Nat. Med. 18. https://doi.org/10.1038/nm.2763.

Barteling, S.J., Woortmeyer, R., 1984. Formaldehyde inactivation of foot-and-mouth disease virus. Conditions for the preparation of safe vaccine. Archives of Virology 80, 103–117. https://doi.org/10.1007/BF01310652.

Bell, J.A., Sundberg, J.P., Ghim, S.J., Newsome, J., Jenson, A.B., Schlegel, R., 1994. A formalin-inactivated vaccine protects against mucosal papillomavirus infection: a canine model. Pathobiology 62. https://doi.org/10.1159/000163910.

Bosch, B.J., van der Zee, R., de Haan, C.A.M., Rottier, P.J.M., 2003. The coronavirus spike protein is a class I virus fusion protein: structural and functional characterization of the fusion core complex. J. Virol. 77, 8801–8811. https://doi.org/10.1128/jvi.77.16.8801-8811.2003.

Chai, K.L., Valk, S.J., Piechotta, V., Kimber, C., Monsef, I., Doree, C., Wood, E.M., Lamikanra, A.A., Roberts, D.J., McQuilten, Z., So-Osman, C., Estcourt, L.J., Skoetz, N., 2020. Convalescent plasma or hyperimmune immunoglobulin for people with COVID-19: a living systematic review. Cochrane Database Syst. Rev. https://doi.org/10.1002/14651858.CD013600.pub3.

Choi, Y., Ahn, C.J., Seong, K.M., Jung, M.Y., Ahn, B.Y., 2003. Inactivated Hantaan virus vaccine derived from suspension culture of Vero cells. Vaccine 21. https://doi.org/10.1016/S0264-410X(03)00005-7.

Chu, C., Qu, K., Zhong, F.L., Artandi, S.E., Chang, H.Y., 2011. Genomic maps of long noncoding RNA occupancy reveal principles of RNA-chromatin interactions. Mol. Cell 44 (4), 667–678. https://doi.org/10.1016/j.molcel.2011.08.027.

Costa, R.N., Abreu, C.L.C., Nascimento, M.C., Nogueira, A.C.M.A., Delgado, I.F., 2010. Evaluation of the applicability of swiss webster lineage on the biological potency test of recombinant human erythropoietin. Int. J. Biosaf. Biosecurity 1, 48–59.

Cubas-Nuñez, L., Duran-Moreno, M., Castillo-Villalba, J., Fuentes-Maestre, J., Casanova, B., García-Verdugo, J.M., Gil-Perotín, S., 2017. In situ RT-PCR optimized

for electron microscopy allows description of subcellular morphology of target mRNA-expressing cells in the brain. Front. Cell. Neurosci. 11. https://doi.org/10.3389/fncel.2017.00141.
da Costa Camila, B.P., Martins, F.J., da Cunha, L.E.R., Ratcliffe, N.A., de Paula, R.C., Castro, H.C., 2021. COVID-19 and Hyperimmune sera: a feasible plan B to fight against coronavirus. Int Immunopharmacol. 90, 1–10. https://doi.org/10.1016/j.intimp.2020.107220.
Dai, L., Gao, G.F., 2021. Viral targets for vaccines against COVID-19. Nat. Rev. Immunol. 21, 73–82. https://doi.org/10.1038/s41577-020-00480-0.
Darnell, M.E.R., Subbarao, K., Feinstone, S.M., Taylor, D.R., 2004. Inactivation of the coronavirus that induces severe acute respiratory syndrome, SARS-CoV. J. Virol. Methods 121, 85–91. https://doi.org/10.1016/j.jviromet.2004.06.006.
Delrue, I., Delputte, P.L., Nauwynck, H.J., 2009. Assessing the functionality of viral entry-associated domains of porcine reproductive and respiratory syndrome virus during inactivation procedures, a potential tool to optimize inactivated vaccines. Vet. Res. 40. https://doi.org/10.1051/vetres/2009047.
Delrue, I., Verzele, D., Madder, A., Nauwynck, H.J., 2012. Inactivated virus vaccines from chemistry to prophylaxis: merits, risks and challenges. Expert Rev. Vaccin. 11, 695–719. https://doi.org/10.1586/erv.12.38.
Dent, S., Neuman, B.W., 2015. Purification of coronavirus virions for Cryo-EM and proteomic analysis. Corona.: Methods Protoc. https://doi.org/10.1007/978-1-4939-2438-7.
Elliott, L.H., McCormick, J.B., Johnson, K.M., 1982. Inactivation of lassa, marburg, and ebola viruses by gamma irradiation. J. Clin. Microbiol. 16 (4), 704–708. https://doi.org/10.1128/jcm.16.4.704-708.1982.
Elveborg, S., Monteil, V.M., Mirazimi, A., 2022. Methods of inactivation of highly pathogenic viruses for molecular, serology or vaccine development purposes. Pathogens 11 (2), 271. https://doi.org/10.3390/pathogens11020271.
Fan, C., Ye, X., Ku, Z., Kong, L., Liu, Q., Xu, C., Cong, Y., Huang, Z., 2017. Beta-propiolactone inactivation of coxsackievirus A16 induces structural alteration and surface modification of viral capsids. J. Virol. 91, e00038–17. https://doi.org/10.1128/jvi.00038-17.
Focosi, D., Franchini, M., 2021. COVID-19 convalescent plasma therapy: hit fast, hit hard! Vox Sang. 116, 935–942. https://doi.org/10.1111/vox.13091.
Fortner, A., Schumacher, D., 2021. First COVID-19 vaccines receiving the US FDA and EMA emergency use authorization. Discoveries 9, e122. https://doi.org/10.15190/d.2021.1.
Furesz, J., Scheifele, D.W., Palkonyay, L., 1995. Safety and effectiveness of the new inactivated hepatitis A virus vaccine. CMAJ.
Furuya, Y., 2012. Return of inactivated whole-virus vaccine for superior efficacy. Immunol. Cell Biol. 90, 571–578. https://doi.org/10.1038/icb.2011.70.
Gao, Q., Bao, L., Mao, H., Wang, L., Xu, K., Yang, M., Li, Yajing, Zhu, Ling, Wang, N., Lv, Z., Gao, H., Ge, X., Kan, B., Hu, Y., Liu, J., Cai, F., Jiang, D., Yin, Y., Qin, Chengfeng, Li, J., Gong, X., Lou, X., Shi, W., Wu, D., Zhang, H., Zhu, Lang, Deng, W., Li, Yurong, Lu, J., Li, C., Wang, X., Yin, W., Zhang, Y., Qin, Chuan, 2020. Development of an inactivated vaccine candidate for SARS-CoV-2. Science 369, 77–81. https://doi.org/10.1016/j.cell.2020.06.008.
Graham, L.L., Beveridge, T.J., 1990. Evaluation of freeze-substitution and conventional embedding protocols for routine electron microscopic processing of eubacteria. J. Bacteriol. 172, 2141–2149. https://doi.org/10.1128/jb.172.4.2141-2149.1990.
Heinz, F., Holtzmann, H., Essl, A., Kundt, M., 2008. Analysis of the efficiency of tick-borne encephalitis vaccination in the population in the natural foci of Austria. Vopr. Virusol. 53.
Herrera-Rodriguez, J., Signorazzi, A., Holtrop, M., de Vries-Idema, J., Huckriede, A., 2019. Inactivated or damaged? Comparing the effect of inactivation methods on influenza virions to optimize. Vaccin. Prod. Vaccin. 37, 1630–1637. https://doi.org/10.1016/j.vaccine.2019.01.086.
Hume, A.J., Ames, J., Rennick, L.J., Duprex, W.P., Marzi, A., Tonkiss, J., Mühlberger, E., 2016. Inactivation of RNA viruses by gamma irradiation: a study on mitigating factors. Viruses 8 (7), 204. https://doi.org/10.3390/v8070204.
International Atomic Energy Agency Convention on the physical protection of nuclear material and nuclear facilities IAEA, 2016. INFCIRC/274/Rev. 1/Mod. 1.
Jiang, W., Schwendeman, S.P., 2000. Formaldehyde-mediated aggregation of protein antigens: comparison of untreated and formalinized model antigens. Biotechnol. Bioeng. 70, 507–517. https://doi.org/10.1002/1097-0290(20001205)70:5<507::AID-BIT5>3.0.CO;2-C.
Ke, Z., Oton, J., Qu, K., Cortese, M., Zila, V., McKeane, L., Nakane, T., Zivanov, J., Neufeldt, C.J., Cerikan, B., Lu, J.M., Peukes, J., Xiong, X., Kräusslich, H.G., Scheres, S.H.W., Bartenschlager, R., Briggs, J.A.G., 2020. Structures and distributions of SARS-CoV-2 spike proteins on intact virions. Nature 588, 498–502. https://doi.org/10.1038/s41586-020-2665-2.
Keles, I., Woldehiwet, Z., Murray, R.D., 1998. Vaccination with glutaraldehyde-fixed bovine respiratory syncytial virus (BRSV)- infected cells stimulates a better immune response in lambs than vaccination with heat-inactivated cell-free BRSV. Vaccine 1172–1178. https://doi.org/10.1016/s0264-410x(98)80116-3.
Kistner, O., Barrett, N., Brühmann, A., Reiter, M., Mundt, W., Savidis-Dacho, H., Schober-Bendixen, S., Dorner, F., Aaskov, J., 2007. The preclinical testing of a formaldehyde inactivated Ross River virus vaccine designed for use in humans. Vaccine 25. https://doi.org/10.1016/j.vaccine.2007.01.103.
Kuo, L., Hurst-Hess, K.R., Koetzner, C.A., Masters, P.S., 2016. Analyses of coronavirus assembly interactions with interspecies membrane and nucleocapsid protein chimeras. J. Virol. 90, 4357–4368. https://doi.org/10.1128/jvi.03212-15.
Le Nedelec, M.J., Rosengren, R.J., 2002. Methylphenidate inhibits cytochrome P450 in the Swiss Webster mouse. Hum. Exp. Toxicol. 21 (5), 273–280. https://doi.org/10.1191/0960327102ht245oa.
Leclercq, S.Y., dos Santos, R.M.M., Macedo, L.B., Campos, P.C., Ferreira, T.C., de Almeida, J.G., Seniuk, J.G.T., Serakides, R., Silva-Cunha, A., Fialho, S.L., 2011. Evaluation of water-in-oil-in-water multiple emulsion and microemulsion as potential adjuvants for immunization with rabies antigen. Eur. J. Pharm. Sci. 43, 378–385. https://doi.org/10.1016/j.ejps.2011.05.008.
Ledford, H., 2021. COVID antibody treatments show promise for preventing severe disease. Nature 591, 513–514. https://doi.org/10.1038/d41586-021-00650-7.
Li, K., Tong, C., Ha, X., Zeng, C., Chen, X., Xu, F., Yang, J., Du, H., Chen, Y., Cai, J., Yang, Z., Jiang, Z., Chai, D., Zhang, X., Li, X., Li, J., Yao, L., 2021. Development and clinical evaluation of a rapid antibody lateral flow assay for the diagnosis of SARS-CoV-2 infection. BMC Infect. Dis. 21, 860. https://doi.org/10.1186/s12879-021-06568-9.
Lu, J.H., Guo, Z.M., Han, W.Y., Wang, G.L., Zhang, D.M., Wang, Y.F., Sun, S.Y., Yang, Q. H., Zheng, H.Y., Wong, B.L., Zhong, N.S., 2005. Preparation and development of equine hyperimmune globulin F(ab') 2 against severe acute respiratory syndrome coronavirus. Acta Pharmacol. Sin. 26, 1479–1484. https://doi.org/10.1111/j.1745-7254.2005.00210.x.
Möller, L., Schünadel, L., Nitsche, A., Schwebke, I., Hanisch, M., Laue, M., 2015. Evaluation of virus inactivation by formaldehyde to enhance biosafety of diagnostic electron microscopy. Viruses 7 (2), 666–679. https://doi.org/10.3390/v7020666.
Pan, X., Zhou, P., Fan, T., Wu, Y., Zhang, J., Shi, X., Shang, W., Fang, L., Jiang, X., Shi, J., Sun, Y., Zhao, S., Gong, R., Chen, Z., Xiao, G., 2020. Immunoglobulin fragment F (ab')2 against RBD potently neutralizes SARS-CoV-2 in vitro. Antivir. Res. 182, 104868 https://doi.org/10.1016/j.antiviral.2020.104868.
Perera, R.A.P.M., Mok, C.K.P., Tsang, O.T.Y., Lv, H., Ko, R.L.W., Wu, N.C., Yuan, M., Leung, W.S., Chan, J.M.C., Chik, T.S.H., Choi, C.Y.C., Leung, K., Chan, K.H., Chan, K. C.K., Li, K.C., Wu, J.T., Wilson, I.A., Monto, A.S., Poon, L.L.M., Peiris, M., 2020. Serological assays for severe acute respiratory syndrome coronavirus 2 (SARS-CoV-2), March 2020. pii=2000421 Eurosurveillance 25. https://doi.org/10.2807/1560-7917.ES.2020.25.16.2000421.
Piechotta, V., Iannizzi, C., Chai, K.L., Valk, S.J., Kimber, C., Dorando, E., Monsef, I., Wood, E.M., Lamikanra, A.A., Roberts, D.J., Mcquilten, Z., So-Osman, C., Estcourt, L. J., Skoetz, N., 2020. Convalescent plasma or hyperimune immunoglobulin for people with COVID-19: a living systematic review (review). Cochrane Database Syst. Rev. 1–398. https://doi.org/10.1002/14651858.CD013600.pub4.www.cochranelibrary.com.
Pollock, R. v, Carmichael, L.E., 1982. Dog response to inactivated canine parvovirus and feline panleukopenia virus vaccines. Cornell Vet. 72, 16–35.
Roberts, A., Lamirande, E.W., Vogel, L., Baras, B., Goossens, G., Knott, I., Chen, J., Ward, J.M., Vassilev, V., Subbarao, K., 2010. Immunogenicity and protective efficacy in mice and hamsters of a β-propiolactone inactivated whole virus SARS-CoV vaccine. Viral Immunol. 23, 509–519. https://doi.org/10.1089/vim.2010.0028.
Rodgers, F.G., Hufton, P., Kurzawska, E., Molloy, C., Morgan, S., 1985. Morphological response of human rotavirus to ultra-violet radiation, heat and disinfectants. J. Med. Microbiol. 20 (1), 123–130. https://doi.org/10.1099/00222615-20-1-123.
Roehrig, J.T., Hombach, J., Barrett, A.D.T., 2008. Guidelines for plaque-reduction neutralization testing of human antibodies to dengue viruses. Viral Immunol. 21, 123–132. https://doi.org/10.1089/vim.2008.0007.
Rossio, J.L., Esser, M.T., Suryanarayana, K., Schneider, D.K., Bess, J.W., Vasquez, G.M., Wiltrout, T.A., Chertova, E., Grimes, M.K., Sattentau, Q., Arthur, L.O., Henderson, L. E., Lifson, J.D., 1998. Inactivation of human immunodeficiency virus type 1 infectivity with preservation of conformational and functional integrity of virion surface proteins. J. Virol. 72, 7992–8001. https://doi.org/10.1128/jvi.72.10.7992-8001.1998.
Sabatini, D.D., Bensch, K., Barrnett, R.J., 1963. Cytochemistry and electron microscopy. The preservation of cellular ultrastructure and enzymatic activity by aldehyde fixation. J. Cell Biol. 17 (1), 19–58. https://doi.org/10.1083/jcb.17.1.19.
Sabbaghi, A., Miri, S.M., Keshavarz, M., Zargar, M., Ghaemi, A., 2019. Inactivation methods for whole influenza vaccine production. Rev. Med. Virol. 29, e2074 https://doi.org/10.1002/rmv.2074.
Salk, J.E., Gori, J.B., 1960. A review of theoretical, experimental, and practical considerations in the use of formaldehyde for the inactivation of poliovirus. Ann. N. Y. Acad. Sci. 83. https://doi.org/10.1111/j.1749-6632.1960.tb40933.x.
Samina, I., Khinich, Y., Simanov, M., Malkinson, M., 2005. An inactivated West Nile virus vaccine for domestic geese-efficacy study and a summary of 4 years of field application. Vaccine 23. https://doi.org/10.1016/j.vaccine.2005.03.052.
Skykes, G., 1965. The theory and mode of action of disinfection, in: Disinfection and Sterilization. LIPPINCOTT, PHILADELPHIA.
Suryadevara, N., Shrihari, S., Gilchuk, P., VanBlargan, L.A., Binshtein, E., Zost, S.J., Nargi, R.S., Sutton, R.E., Winkler, E.S., Chen, E.C., Fouch, M.E., Davidson, E., Doranz, B.J., Chen, R.E., Shi, P.Y., Carnahan, R.H., Thackray, L.B., Diamond, M.S., Crowe, J.E., 2021. Neutralizing and protective human monoclonal antibodies recognizing the N-terminal domain of the SARS-CoV-2 spike protein. Cell 184 (2316–2331), e15. https://doi.org/10.1016/j.cell.2021.03.029.
Tano, Y., Shimizu, H., Martin, J., Nishimura, Y., Simizu, B., Miyamura, T., 2007. Antigenic characterization of a formalin-inactivated poliovirus vaccine derived from live-attenuated Sabin strains. Vaccine 25, 7041–7046. https://doi.org/10.1016/j.vaccine.2007.07.060.
Tsai, S.C., Lu, C.C., Bau, D.T., Chiu, Y.J., Yen, Y.T., Hsu, Y.M., Fu, C.W., Kuo, S.C., Lo, Y. S., Chiu, H.Y., Juan, Y.N., Tsai, F.J., Yang, J.S., 2021. Approaches towards fighting the COVID-19 pandemic (review). Int. J. Mol. Med. 47, 3–22. https://doi.org/10.3892/ijmm.2020.4794.
Tuttle, A.H., Philip, V.M., Chesler, E.J., Jeffrey, S., Mogil, J.S., 2018. Comparing phenotypic variation between inbred and outbred mice. Nat. Methods 15, 994–996. https://doi.org/10.1038/s41592-018-0224-7.

Uittenbogaard, J.P., Zomer, B., Hoogerhout, P., Metz, B., 2011. Reactions of β-propiolactone with nucleobase analogues, nucleosides, and peptides: implications for the inactivation of viruses. J. Biol. Chem. 286, 36198–36214. https://doi.org/10.1074/jbc.M111.279232.

Valko, M., Leibfritz, D., Moncol, J., Cronin, M.T., Mazur, M., Telser, J., 2007. Free radicals and antioxidants in normal physiological functions and human disease. Int. J. Biochem. Cell Biol. 39 (1), 44–84. https://doi.org/10.1016/j.biocel.2006.07.001.

Vanhove, B., Duvaux, O., Rousse, J., Royer, P.J., Evanno, G., Ciron, C., Lheriteau, E., Vacher, L., Gervois, N., Oger, R., Jacques, Y., Conchon, S., Salama, A., Duchi, R., Lagutina, I., Perota, A., Delahaut, P., Ledure, M., Paulus, M., So, R.T., Mok, C.K.P., Bruzzone, R., Bouillet, M., Brouard, S., Cozzi, E., Galli, C., Blanchard, D., Bach, J.M., Soulillou, J.P., 2021. High neutralizing potency of swine glyco-humanized polyclonal antibodies against SARS-CoV-2. Eur. J. Immunol. 51, 1412–1422. https://doi.org/10.1002/eji.202049072.

Wang, C., Xiao, X., Feng, H., Hong, Z., Li, M., Tu, N., Li, X., Wang, K., Bu, L., 2021. Ongoing COVID-19 pandemic: a concise but updated comprehensive review. Curr. Microbiol. 78, 1718–1729. https://doi.org/10.1007/s00284-021-02413-z.

Yeh, K.B., Tabynov, K., Parekh, F.K., Mombo, I., Parker, K., Tabynov, K., Bradrick, S.S., Tseng, A.S., Yang, J., Gardiner, L., Olinger, G., Setser, B., 2021. Significance of high-containment biological laboratories performing work during the COVID-19 pandemic: biosafety level-3 and -4 labs. Front. Bioeng. Biotechnol. 9, 720315 https://doi.org/10.3389/fbioe.2021.720315.